ARTICLE IN PRESS

International Journal of Transportation Science and Technology xxx (xxxx) xxx

Contents lists available at ScienceDirect

International Journal of Transportation Science and Technology

journal homepage: www.elsevier.com/locate/ijtst

Research Paper

An analytical model of many-to-one carpool system performance under cost-based detour limits

Xin Dong, Hao Liu *, Vikash V. Gayah

Department of Civil and Environmental Engineering, The Pennsylvania State University, University Park, PA 16802, USA

ARTICLE INFO

Article history:
Received 25 January 2024
Received in revised form 4 April 2024
Accepted 26 May 2024
Available online xxxx

Keywords:
Many-to-one
Carpool system
Cost-based detour limits
Flexible-role

ABSTRACT

Carpooling has emerged as a highly efficient method for mitigating traffic congestion. By strategically consolidating multiple travelers into fewer vehicles, carpooling substantially cuts down the overall number of vehicles on the road. However, the effectiveness of a carpooling system highly depends on the proportion of interested users that can be successfully matched and the amount of benefits users gain from these matches. This paper develops analytical models to estimate these metrics for a carpooling system that serves a many-to-one demand pattern, in which travelers share the same basic destination but travel from different origins. Two distinct scenarios are incorporated in the models: one where users have a preferred role of a driver or rider and another in which they are ambivalent between the two roles. The models provide the system's expected match rate and average user surplus as a function of the network size, number of users, and travel costs. Different from previous studies, the proposed models developed here consider that users only participate in trips that are beneficial to them from a cost perspective, rather than assuming fixed detours. This allows for matching incorporating spatial and financial considerations, promising flexible and rational matches in carpool systems. Simulation tests are used to validate the effectiveness of the analytical models. Results also offer insights into how various factors impact the system's performance.

1. Introduction

Continually expanding roadway networks and building new infrastructure are not efficient solutions to alleviate congestion and address environmental concerns associated with automobile transportation. For one, space for transportation infrastructure is limited. Further, these approaches can create more travel demand – a phenomenon termed 'induced demand' as highlighted by Cervero (2003) – that worsens the problem. An alternative solution is to decrease the number of vehicles traveling by increasing the passenger occupancy rate of each vehicle. With the increase in the popularity of shared mobility in urban transportation networks, carpooling has become a commonly proposed travel mode to help reach this goal. Different from ridesharing, which usually includes not only travelers but also a dedicated driver, carpooling is a self-scheduling mode in which travelers agree to share their trips without the need for extra drivers, as explained by Handke and Jonuschat (2012). Olsson et al. (2019) noted that carpooling emerged in the United States in the 1970s as a solution to the growing oil crisis; however, carpool demand declined after that time and tended to resurface during periods of

* Corresponding author.
E-mail address: hfl5376@psu.edu (H. Liu).

https://doi.org/10.1016/j.ijtst.2024.05.007

Please cite this article as: X. Dong, H. Liu and V.V. Gayah, An analytical model of many-to-one carpool system performance under cost-based detour limits, International Journal of Transportation Science and Technology, https://doi.org/10.1016/j.ijtst.2024.05.007

increased travel costs such as the oil crises in 2005 and financial crises in 2008. Thanks to the boom of the internet and the sharing economy, carpooling has been boosted rapidly recently, as detailed by Furuhata et al. (2013).

The financial benefits and improvements in operational efficiency have drawn abundant research efforts as critical factors considered by stakeholders for the investment in the carpool system. Numerous studies have explored how various factors influence the performance of carpool systems – for example, Lehe et al. (2021), Liu et al. (2023) have investigated how demand affects carpool systems; Regue et al. (2016), Zhang et al. (2014) focused on the impact of system design; Zhang et al. (2013) analyzed the effects of pricing strategies; and Daganzo et al. (2020), Wang et al. (2021), Ouyang et al. (2021) examined the role of detour or waiting time policies. Furthermore, the influence of matching algorithms has been explored by Xia et al. (2015), Masoud and Jayakrishnan (2017a), Tafreshian and Masoud (2020), on the performance of carpool systems.

Several studies explored the influencing factors of the carpool system or ride-splitting system's performance using big data. Lehe et al. (2021) used data from the carpool service (Scoop) to identify signs of increasing returns to scale in a carpool matching system; specifically, as more participants join the carpool system, there is a greater potential for enhanced matching performance and overall benefits. Liu et al. (2023) utilized ridesharing data from Chicago to demonstrate how an increase in requested shared trips leads to higher matching rates and reduced detour distances. Some agent-based models were also conducted, which simulated the whole carpool process to reproduce the real scene and explore the influence of certain factors for optimization: For example, Masoud and Jayakrishnan (2017b) modeled the carpool system as a bipartite graph and developed a ride-matching algorithm, in which they used a rolling time horizon framework to increase the matching rate. Huang et al. (2014) proposed a genetic algorithm to solve the multi-objective optimization problem in the carpool system, which helps increase matched passengers and is more efficient. Zhang et al. (2019) presented a multi-objective optimization model to find the best pricing parameters that protect both the drivers' and the riders' benefits from carpooling by taxi.

Although these data-based and agent-based studies are very detailed and provide precise estimates of performance, they usually require a large amount of input data – such as individual preferences, information on operated vehicles, trip itineraries, etc. – which usually are challenging to obtain and time-consuming to process and simulate. In comparison, analytical models that require less detailed input data have been developed to obtain more general, but less precise, insights about the carpooling system's performance. For example, Daganzo and Ouyang (2019) derived a general analytical model to quantify the cost and performance of dial-a-ride ride-sharing systems, which considers the system status and dynamics. However, the detour distance – the additional distance people may travel to facilitate a carpool – in this model can be infinite. Other models have been proposed to address this issue. Daganzo et al. (2020) developed closed-form formulas using system dynamics to quantify the performance of ridesharing with upper limits of detours and proved that taxis produce shorter trip times than the case without limits. Wang et al. (2021) proposed a model that can predict the matching probability, expected detour, and shared distance for each passenger. This model can be used by carpool companies to predict the profit and develop discount policies to attract riders. Ouyang et al. (2021) established a many-to-many carpool analytical model with fixed detour limits and waiting time restrictions. The proposed model can predict the performance of the carpool system in terms of Vehicle Kilometers Traveled (VKT), and Personal Kilometers Traveled (PKT) in idealized settings accurately.

These previous analytical studies assumed that carpool users can be potentially matched as long as detours are within some fixed distance limit (i.e., assume a fixed maximum detour distance to create a carpool); however, this assumption is questionable in practice. For instance, if some passengers have very short trip distances, and the assigned drivers experience a quite large detour distance, they may not be willing to carpool if payment by the rider does not adequately cover the additional costs incurred due to the detour. In such cases, carpooling would create a negative surplus and increase the total travel cost. Therefore, it's plausible to assume that a driver's acceptable detour distance hinges on the monetary benefits from matching, and varies with trip-specific factors like origin, destination, and payment rates. Incorporating such consideration, we developed an analytical model to evaluate carpool systems' performance (including match rate and financial benefits) with a many-to-one demand pattern, particularly emulating morning commutes from various suburban locations to a Central Business District (CBD). Given that only 8.8% of commuters carpool according to the U.S. Census Bureau (2022), we concentrate on 'small' carpooling systems with relatively few people willing to carpool. Specifically, the contributions of this paper include: (1) account for individual variations in acceptable detour distance, taking into consideration travel costs; (2) consider scenarios with both fixed-role and flexible-role participants; (3) investigate the impact of demand, payment-cost ratio, driver-rider ratio, and role flexibility on the carpool system's performance; and, (4) demonstrate the accuracy of our findings from the proposed analytical models via simulation.

The remainder of this paper is organized as follows. The subsequent section provides a detailed description of the realistic scenarios in which this model is applied. Following that, the next section delves into the methodology employed to evaluate the performance of the carpool system. The numerical validation of the analytical model is presented in the next section. The following section presents a thorough analysis of the impact of certain factors on the carpool system's performance using models derived from the study. Finally, the key takeaways and concluding remarks are provided.

2. Scenario

This paper considers a 'many-to-one' scenario in which trip origins are homogeneously distributed across a large region but ultimately destined for the same location. This is a typical phenomenon for urban cities in which commuters across the entire city travel to the downtown region during morning peak hours. Such demand pattern has been widely used in the literature (Lam and Huang (1995), Wang et al. (2015), Su and Wang (2020), Tian et al. (2021), Mortazavi et al. (2024)). In this scenario, the following assumptions are made and applied to all the proposed models: (1) settings with a dense grid-like street network are considered; (2) origins of travel demand are homogeneously distributed; (3) all travelers take the Manhattan distance-based shortest path to their destination; (4) travelers can take either one or both of two roles: a driver or a rider; (5) at most two people can travel together in a carpool trip; (6) riders reimburse drivers for the trips, and the rate of this reimbursement is smaller than the rate of traveling alone; and, (7) riders who fail to be matched to a driver are able to drive alone to the destination. The fifth assumption is widely accepted and frequently employed, for instance, Ouyang et al. (2021) utilized the two-person carpool assumption in their analytical model; Xia et al. (2015) conducted a survey, and claimed that 13.3% of participants were involved in two-person carpools, 4.4% in three-person carpools, and 2.3% participated in van-pool services. After the carpool requests are sent by users, the system will assign carpool pairs based on whether the shared trip is financially beneficial for both, as will be described later in this section.

2.1. Many-to-one environment

The 'many-to-one' environment is common for urban transportation networks; e.g., commuters from all over a city travel towards a dense downtown region during morning peak hours. Fig. 1(a) presents the comprehensive future land use plan of Washington, D.C., developed with data from OpenDataDC (2023), which serves as an example of the 'many-to-one' environment. In this environment, it is expected that the central high-density commercial region (red-colored) will attract commuters from the surrounding residential areas (yellow-colored) during peak hours. In the analytical model, we considered the environment with a grid-like street layout as a $2l(km) \times 2l(km)$ square region with area A, as shown in Fig. 1(b). The destinations are located at the center of the region with coordinates $(0, 0)$, shown by the red dot; the origins of commuters are uniformly distributed from the whole area, examples are shown by the green and blue dots.

2.2. Trip routing and trip distance

For the network configuration shown in Fig. 1(b), the L_1 (or Manhattan) metric is employed to calculate the travel distance for all trips. The blue and green routes in Fig. 1(b) are two feasible routes for travelers originating from the blue and green dots if they travel alone. The trip distance for the driver and the rider when traveling alone can be expressed as $L_d = |X_d| + |Y_d|$ and $L_r = |X_r| + |Y_r|$, respectively. The yellow route shows a feasible path under pooling scenario if a driver

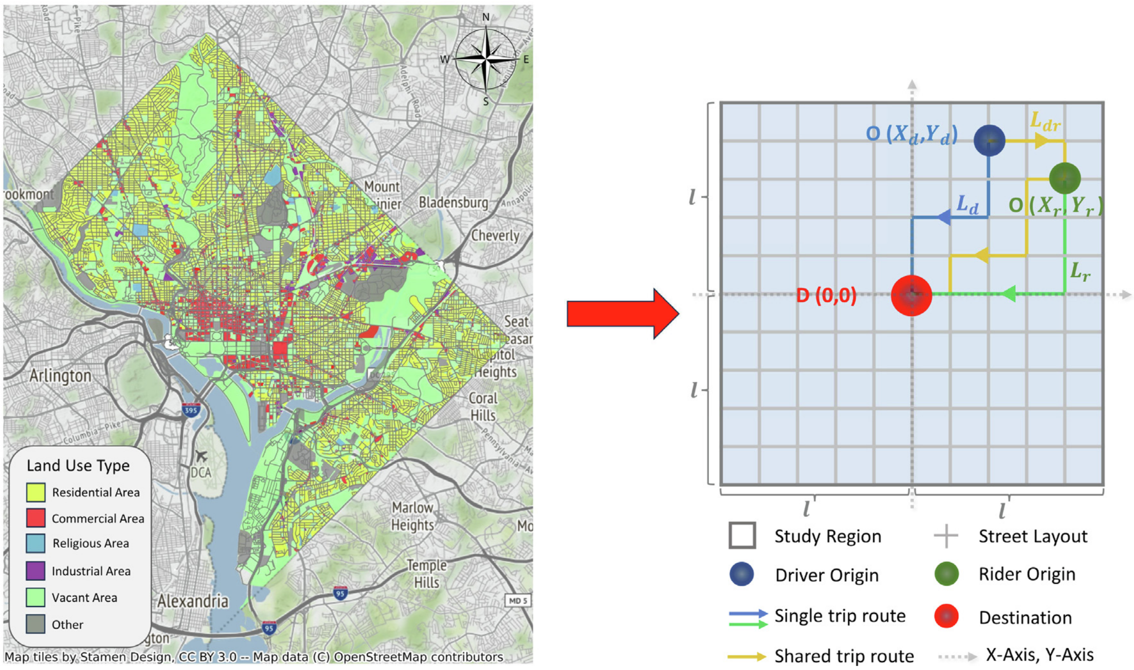

(a) **Washington D.C. Layout and Land Use** (b) **An example network of the Analytical Model**

Fig. 1. Many-to-one carpooling environment setting.

at (X_d, Y_d) matched with a rider at (X_r, Y_r). This trip consists of two parts: (1) the trip from the driver's origin, O_d, to the rider's origin, O_r, with a length of L_{dr}; and, (2) the trip from the rider's origin O_r to their destination $D(0,0)$ with a length of L_r. Compared to driving alone, the extra travel distance incurred by the driver, L_{dt}, is referred to as detour distance. L_{dr} and L_{dt} can be expressed as:

$$L_{dr} = |X_d - X_r| + |Y_d - Y_r|. \tag{1}$$

$$L_{dt} = L_{dr} + L_r - L_d = |X_d - X_r| + |Y_d - Y_r| + (|X_r| + |Y_r|) - (|X_d| + |Y_d|). \tag{2}$$

2.3. Trip cost

For ease of calculation, we estimate trip costs based on a fixed unit cost per distance, $\alpha(\$/km)$, with the rider reimbursement rate as $\beta(\$/km)$, and set β less than α. We also define the ratio of $\gamma = \beta/\alpha$ as the payment-cost ratio, which represents the relationship between the payment and cost rate. It's important to highlight that $\beta \leqslant \alpha$, which ensures $0 < \gamma \leqslant 1$, indicates that the unit cost of being involved in a carpool pair is less than driving alone. Therefore, various types of expenses involved can be expressed with all the rates and trip distances in the following equations:

$$C_d^a = \alpha L_d = \alpha(|X_d| + |Y_d|), \tag{3}$$

$$C_d^p = \alpha(L_{dr} + L_r) - \beta L_r = \alpha(|X_d - X_r| + |Y_d - Y_r| + |X_r| + |Y_r|) - \beta(|X_r| + |Y_r|), \tag{4}$$

$$C_r^a = \alpha L_r = \alpha(|X_r| + |Y_r|), \tag{5}$$

$$C_r^p = \beta L_r = \beta(|X_r| + |Y_r|), \tag{6}$$

where C_d^a is the cost a driver incurs without picking up a rider; C_d^p is the cost the driver incurs when picking up a rider, including all detours and reimbursements; C_r^a is the cost the rider incurs if they were to drive themselves; and, C_r^p is the cost the rider incurs in a pooled trip.

2.4. Surplus

We define the cost savings achieved through carpooling compared to the scenario where individuals travel alone as the 'surplus', which can be used to evaluate the economic benefits produced by the carpool system. The surplus for the driver, S_d, and the rider, S_r, can be expressed as:

$$\begin{aligned} S_d &= C_d^a - C_d^p = \alpha L_d - [\alpha(L_{dr} + L_r) - \beta L_r] = \beta L_r - \alpha(L_{dr} + L_r - L_d) \\ &= \alpha(|X_d| + |Y_d|) - (|X_d - X_r| + |Y_d - Y_r|)) - (\alpha - \beta)(|X_r| + |Y_r|). \end{aligned} \tag{7}$$

$$S_r = C_r^a - C_r^p = \alpha L_r - \beta L_r = (\alpha - \beta)(|X_r| + |Y_r|). \tag{8}$$

Also, we use $S(X_r, Y_r, X_d, Y_d)$ to refer to the combined surplus of the driver and the rider in a carpool pair (i.e., $S_d + S_r$). It is dependent on the locations of the driver and the rider, and can be expressed as:

$$S(X_r, Y_r, X_d, Y_d) = S_d + S_r = \alpha(|X_d| + |Y_d| - |X_r - X_d| - |Y_r - Y_d|). \tag{9}$$

2.5. Financially-feasible matching rule

A financially feasible matching rule is proposed based on the notion of individual rationality in the carpooling system. The carpool system collects all trips that occur within a period (e.g., 5 min) and pairs travelers within with the matching rule. This rule ensures that carpool pairs would only form when both individuals benefit from the match.

Mathematically, this means that carpools only form if $S_r \geqslant 0$ and $S_d \geqslant 0$, and this also promises $S(X_r, Y_r, X_d, Y_d) \geqslant 0$. Under our setting, engaging in a carpool pair is always financially beneficial for riders, $S_r \geqslant 0$, when $\beta \leqslant \alpha$. However, the drivers will only engage in a pair if the extra cost incurred from the detour can be reimbursed by the rider's payment, which is $S_d \geqslant 0$.

Compared to a prevalent assumption in the literature that drivers are willing to travel with fixed detour limits, implying a uniform value for all – as seen in the work of Ouyang et al. (2021), Lin et al. (2012), Zhang et al. (2019)) – denoted by Δ, the cost-based detour limits (varying value for everyone) in our rule is more realistic.

The fixed detour tolerance assumption requires $L_{dt} \in [0, \Delta]$, which results in the surplus of the pair, $S(X_r, Y_r, X_d, Y_d)$ falls in the range of $[\alpha(L_r - \Delta), \alpha L_r]$, as derived by Equation (10). Under this scenario, the surplus can be negative if $L_r < \Delta$. A simple example is when the fixed detour distance tolerance, Δ, is 1 mile, however, one rider's trip distance, L_r, is 0.8 mile, then there is a budget deficiency for the driver, and it is highly unlikely that the driver would pick up the rider in reality. Thus, the fixed detour tolerance is not always financially feasible. However, we require the carpool pair forms only if $S(X_r, Y_r, X_d, Y_d) \geqslant 0$

hold. Therefore, the mechanism we proposed provides a more rational way of carpool matching, where every participant would find it financially beneficial to join, and promises individual rationality and a self-sustaining carpool system.

$$\begin{aligned} S(X_r, Y_r, X_d, Y_d) &= S_d + S_r = [\beta L_r - \alpha(L_{dr} + L_r - L_d)] + [\alpha L_r - \beta L_r] \\ &= \alpha(L_d - L_{dr}) = \alpha(L_r - L_{dt}) \in [\alpha(L_r - \Delta), \alpha L_r]. \end{aligned} \tag{10}$$

3. Analytical model

In this section, we derive analytical models to estimate the performance of the proposed carpool system under various conditions. The intuition is to provide realistic estimates of the system match rate and surplus by using system-level statistics and ignoring individual-level information. Two scenarios are considered: (1) a fixed-role scenario in which each traveler can only take a single role (either driver or rider); and, (2) a flexible-role scenario in which travelers can be assigned as either of both roles. The fixed-role scenario represents a situation more commonly encountered in reality, where each user's role is predetermined. Conversely, the flexible-role scenario, though less prevalent, is posited as a more optimal operating mode that the study aims to substantiate and advocate for, in comparison to the fixed-role approach. The influential factors considered in the models include trip demand, as well as the payment-cost ratio, γ.

3.1. Feasible region for a rider

We first explore the set of locations in which a driver would be financially motivated to pick up a specific rider. This collection of locations is designated as the feasible region for the rider, referred to as $\Omega_r(X_r, Y_r)$. The area of this region is defined as $A_f(X_r, Y_r)$.

Since the network is symmetric and the travelers are assumed to be homogeneously distributed in the network, to simplify calculations without loss of generality, we consider the situation where the rider is in the first quadrant, i.e., $X_r \geqslant 0$ and $Y_r \geqslant 0$, at the same time, consider the drivers are located throughout the whole network, i.e., $-l \leqslant X_d \leqslant l$ and $-l \leqslant Y_d \leqslant l$. Therefore, the feasible region for a given rider located at (X_r, Y_r) can be expressed as:

$$\Omega_r(X_r, Y_r) = \{(X_d, Y_d) | (|X_r - X_d| + |Y_r - Y_d|) - (|X_d| + |Y_d|) + (1 - \gamma) * (X_r + Y_r) \leqslant 0\}, \tag{11}$$

which is derived from Eq. (7) by ensuring the non-negativity of S_d.

Because of the existence of the absolute value signs (ABS) in Eq. (11), we need to express the boundary of the feasible region case-by-case. Since there are 4 ABS, removing these operators would result in 2^4 cases, however, only 8 of them exist. For instance, the case where $X_d < 0, Y_d < 0, X_d - X_r > 0$, and $Y_d - Y_r > 0$ does not exist, since $X_r > 0$ and $Y_r > 0$. Then we define each of the 8 cases as a feasible sub-region. The feasible region of the rider at (X_r, Y_r) is correspondingly partitioned into eight sub-regions $\Omega_{r,i}(X_r, Y_r)$, $i = 1, 2, \ldots, 8$.

Some features of the feasible region could be achieved as a function of the locations of the rider and the size of the region, denoted as $f(x_r, y_r, l)$. Table1 presents these features as the rider's location in the first column, the boundary of each sub-region in the second column, the area of each sub-region in the third column, and the overall surplus within each sub-region in the fourth column. The boundary of each sub-region varies according to the rider's location, (X_r, Y_r), and is determined by multiple inequalities. Consequently, binding inequalities need to be discussed, which explains the existence of multiple situations within each cell of Table1.

Table 1
Feasible drivers attributes for a rider.

i	Location of (x_r, y_r)	$\Omega_{r,i}$ expressed by (X_d, Y_d)	$A_{f,i}(x_r, y_r)$	$\iint_{\Omega_{r,i}(x_r,y_r)} S(x_r, y_r, x_d, y_d)$
1	$x_r \in [0, l], y_r \in [0, l]$	$X_d \in [x_r, l], \quad Y_d \in [y_r, l]$	$(l - x_r)(l - y_r)$	$\alpha(x_r + y_r)(l - x_r)(l - y_r)$
2	$x_r \in [0, l], y_r \in [0, l]$ i. $y_r \geqslant \frac{\gamma}{2-\gamma} x_r$ ii. $y_r \leqslant \frac{\gamma}{2-\gamma} x_r$	$X_d \in [x_r, l]$, $Y_d \in \left[\frac{(2-\gamma)}{2} y_r - \frac{\gamma}{2} x_r, y_r\right]$	i. $\frac{\gamma}{2}(l - x_r)(x_r + y_r)$ ii. $(l - x_r) y_r$	i. $\frac{\alpha\gamma(2-\gamma)}{4}(x_r + y_r)^2(l - x_r)$ ii. $\alpha(l - x_r) x_r y_r$
3	$x_r \in [0, l], y_r \in [0, l]$ i. $x_r \geqslant \frac{\gamma}{2-\gamma} y_r$ ii. $x_r \leqslant \frac{\gamma}{2-\gamma} y_r$	$X_d \in \left[\frac{(2-\gamma)}{2} x_r - \frac{\gamma}{2} y_r, x_r\right]$, $Y_d \in [y_r, l]$	i. $\frac{\gamma}{2}(l - y_r)(x_r + y_r)$ ii. $(l - y_r) x_r$	i. $\frac{\alpha\gamma(2-\gamma)}{4}(x_r + y_r)^2(l - y_r)$ ii. $\alpha(l - y_r) x_r y_r$.
4	$x_r \in [0, l], y_r \in [0, l]$ i. $y_r \geqslant \frac{2-\gamma}{\gamma} x_r$ ii. $\frac{\gamma}{2-\gamma} x_r \leqslant y_r \leqslant \frac{2-\gamma}{\gamma} x_r$ iii. $y_r \leqslant \frac{\gamma}{2-\gamma} x_r$	$X_d \in [0, x_r], \quad Y_d \in [0, y_r]$, $(X_d + Y_d) \geqslant \frac{2-\gamma}{2}(x_r + y_r)$	i. $\frac{1}{2} x_r [(\gamma - 1) x_r + \gamma y_r]$ ii. $\frac{\gamma^2}{8}(x_r + y_r)^2$ iii. $\frac{1}{2} y_r [\gamma x_r + (\gamma - 1) y_r]$	i. $\frac{(6\gamma - 3\gamma^2 - 2)}{12} x_r^3 - \frac{(1-\gamma)^2}{2} x_r^2 y_r + \frac{\gamma(2-\gamma)}{4} x_r y_r^2$ ii. $\frac{\alpha\gamma(3\gamma - 2\gamma^2)}{24A}(x_r + y_r)^3$ iii. $\frac{(6\gamma - 3\gamma^2 - 2)}{12} y_r^3 - \frac{(1-\gamma)^2}{2} y_r^2 x_r + \frac{\gamma(2-\gamma)}{4} y_r x_r^2$
5	$x_r \in [0, l], y_r \in \left[0, \frac{\gamma}{2-\gamma} x_r\right]$	$X_d \in [x_r, l], \quad Y_d \in [-l, 0]$	$(l - x_r) l$	$\alpha l (l - x_r)(x_r - y_r)$
6	$x_r \in \left[0, \frac{\gamma}{2-\gamma} y_r\right], y_r \in [0, l]$	$X_d \in [-l, 0], \quad Y_d \in [y_r, l]$	$(l - y_r) l$	$\alpha l (l - y_r)(y_r - x_r)$
7	$x_r \in [0, l], y_r \in \left[0, \frac{\gamma}{2-\gamma} x_r\right]$	$X_d \in [0, x_r], \quad Y_d \in [-l, 0]$	$\left[\frac{\gamma}{2} x_r - \frac{(2-\gamma)}{2} y_r\right] l$	$\alpha l \left[\frac{\gamma(2-\gamma)}{4}(y_r + x_r)^2 - x_r y_r\right]$
8	$x_r \in \left[0, \frac{\gamma}{2-\gamma} y_r\right], y_r \in [0, l]$	$X_d \in [-l, 0], \quad Y_d \in [0, y_r]$	$\left[\frac{\gamma}{2} y_r - \frac{(2-\gamma)}{2} x_r\right] l$	$\alpha l \left[\frac{\gamma(2-\gamma)}{4}(y_r + x_r)^2 - x_r y_r\right]$

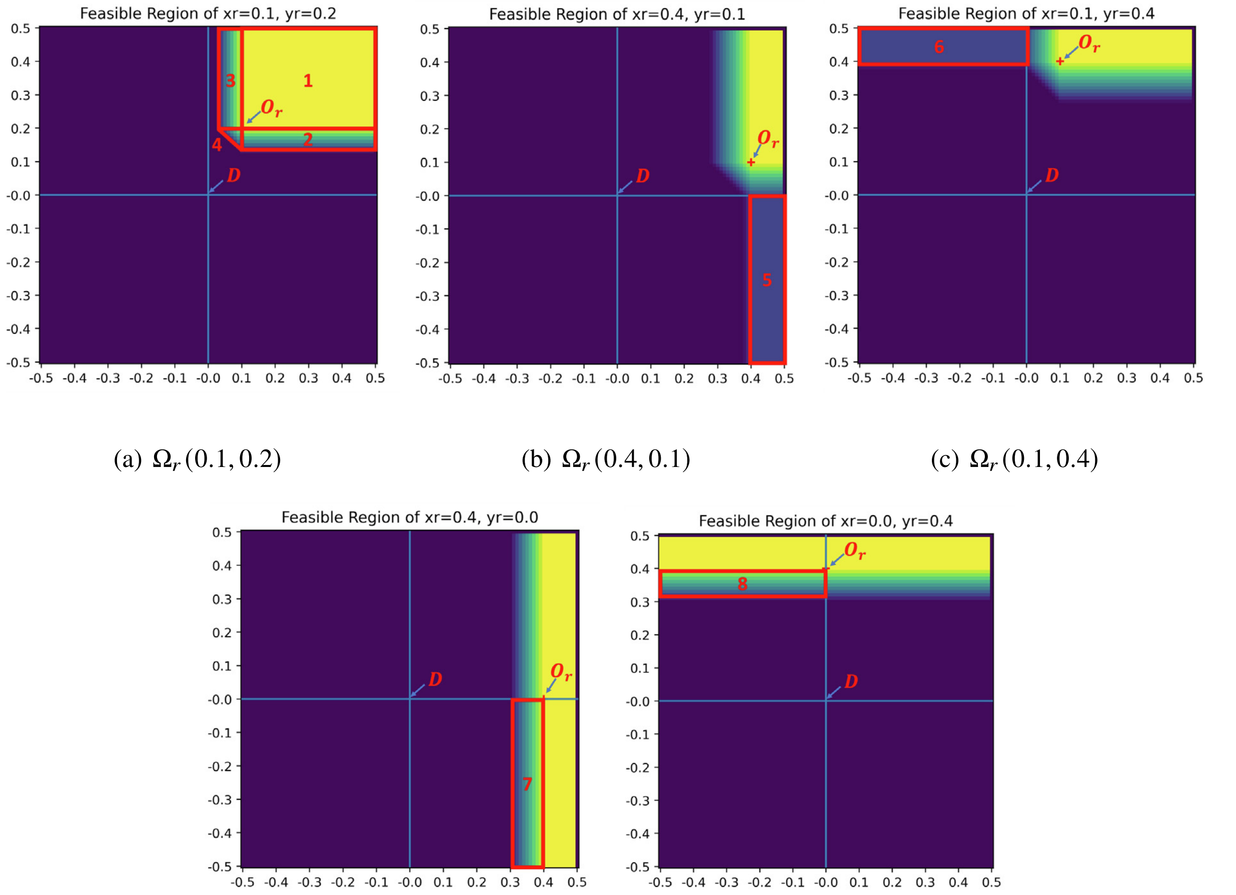

(a) $\Omega_r(0.1, 0.2)$ (b) $\Omega_r(0.4, 0.1)$ (c) $\Omega_r(0.1, 0.4)$

(d) $\Omega_r(0.4, 0)$ (e) $\Omega_r(0, 0.4)$

Fig. 2. Feasible regions (Ω_r) at different locations (Sub-regions 1–4 exist at all (x_r, y_r)s, while sub-regions 5–8 only exist at certain (x_r, y_r)s.).

To facilitate a better understanding of these variations, some feasible regions of certain rider locations are visualized in Fig. 2. An example rider with location $(0.1, 0.2)$ is depicted in Fig. 2(a), where the labeled sub-regions 1–4 have features listed in the $i^{th}(i = 1, 2, 3, 4)$ row of Table1. Find the Roman numeral (i., ii., iii.) corresponding to the inequality that (X_r, Y_r) satisfies, and then the above-mentioned features can be calculated using the formulas in corresponding columns with the same Roman numerals. It is obvious in Table 1 that sub-regions 1–4 are present for every origin of the rider, whereas sub-regions 5–8, illustrated in Fig. 2(b) - Fig. 2(e), are specific to certain rider origins restricted by conditions shown in the 1^{st} column in Table 1.

For subsequent analysis, the area of the feasible region conditional on (x_r, y_r), expressed as $A_f(x_r, y_r) = \sum_{i=1}^{8} A_{f,i}(x_r, y_r)$, and the expected surplus conditional on (x_r, y_r), $\bar{S}_{x_r y_r}$, expressed in Eq. (12) are crucial components for the analytical models to get both the match rate and the system surplus.

$$\bar{S}_{x_r y_r} = \sum_{i=1}^{8} \iint_{\Omega_{r,i}(x_r, y_r)} f_{X_d, Y_d}(x_d, y_d) S(x_r, y_r, x_d, y_d)\, dx_d dy_d, \tag{12}$$

where $f_{X_d, Y_d}(x_d, y_d)$ is the probability density function (PDF) of the location of all feasible drivers. However, all the closed-form formulas in Table1 and results in the following sections are provided with $f_{X_d, Y_d}(x_d, y_d)$ in the form of uniform distribution, denoted as $\frac{1}{A_f(x_r, y_r)}$, for the sake of mathematical tractability. The integration results of surplus over segmented sub-regions are provided in Table1.

3.2. Fixed-role carpool system

This section derives models to estimate the performance of the carpool system when drivers and riders have pre-registered roles. This may exist when each person selects the type of role they wish to perform (either rider or driver) before the matching process.

3.2.1. Special case: single rider

First, a special case in which only a single rider exists is provided. This is then applied and advanced to a more general case when n_r riders are present.

Match Rate

System match rate is defined as the ratio of travelers – both riders and drivers – who are successfully paired. This measure can be derived from the probability of a rider finding a match.

The probability that a single rider successfully matches with the existence of n_d drivers, denoted as $p_r(1, n_d)$, is determined by the likelihood of at least one driver being within the region $\Omega_r(X_r, Y_r)$. Let N_Ω represent the count of drivers within $\Omega_r(X_r, Y_r)$. Then, $p_r(1, n_d)$ is defined as the probability that $N_\Omega \geqslant 0$, given coordinates $(X_r = x_r, Y_r = y_r)$. Thus, the expected value of $p_r(1, n_d)$, denoted as $\bar{p}_r(1, n_d)$, can be expressed as follows:

$$\begin{aligned}\bar{p}_r(1,n_d) &= \bar{p}(N_\Omega \geqslant 0) = \iint_{A_1} p(X_r = x_r, Y_r = y_r) p(N_\Omega \geqslant 0 | X_r = x_r, Y_r = y_r)\, dx_r dy_r \\ &= \int_0^{\frac{\sqrt{A}}{2}} \int_0^{\frac{\sqrt{A}}{2}} f_{X_r,Y_r}(x_r, y_r) \left[1 - \left(1 - \iint_{\Omega_r(x_r,y_r)} f_{X_d,Y_d}(x_d, y_d) dx_d dy_d\right)^{n_d}\right] dx_r dy_r,\end{aligned} \tag{13}$$

where A_1 is the first quadrant where all possible $(x_r, y_r)s$ distributed; $p(N_\Omega \geqslant 0 | X_r = x_r, Y_r = y_r)$, can be expressed with $A_f(x_r, y_r)$, provided in Table 1. $f_{X_r,Y_r}(x_r, y_r)$ is the PDF of riders, in further discussion, we replace this PDF with $\frac{4}{A}$, considering the homogeneously distributed demand of riders in the 1^{st} quadrant. The inner integration yields the probability of falling inside the feasible region of a specific rider.

And therefore the system match rate when there are 1 rider and n_d drivers, denoted as $\bar{p}_{sys}(1, n_d)$, can be formulated as:

$$\bar{p}_{sys}(1, n_d) = \frac{2\bar{p}_r(1, n_d)}{(1 + n_d)}. \tag{14}$$

System Surplus

The system surplus, encompassing both matched and unmatched participants, is the surplus collected from matched pairs divided by the total number of participants in the system. The collected surplus is obtained by multiplying the count of riders with the expected surplus of a pair that the rider is involved in, determined by integrating over all locations ($(x_r, y_r)s$ and $(x_d, y_d)s$). Note if the rider is not involved in any pairs, the surplus for the 'pair' is 0. The integration to determine the expected surplus of a pair is performed in two steps: First, a weighted sum of the surplus for a specific rider across all driver locations, denoted as $\bar{S}_{x_r y_r}$, is calculated as shown in Eq. (12). Second, take a weighted sum of $\bar{S}_{x_r y_r}$ across all potential rider locations.

Therefore, for this special case of 1 rider and n_d drivers, the system surplus, denoted as $\bar{S}_{sys}(1, n_d)$, is expressed as:

$$\begin{aligned}\bar{S}_{sys}(1,n_d) &= \tfrac{1}{(1+n_d)} \iint_{A_1} p(X_r = x_r, Y_r = y_r) \bar{S}_{x_r y_r} p(N_\Omega \geqslant 0 | X_r = x_r, Y_r = y_r)\, dx_r dy_r \\ &= \tfrac{1}{(1+n_d)} \iint_{A_1} f_{X_r,Y_r}(x_r, y_r)\, \bar{S}_{x_r y_r} \left[1 - \left(1 - \iint_{\Omega_r(x_r,y_r)} f_{X_d,Y_d}(x_d, y_d) dx_d dy_d\right)^{n_d}\right] dx_r dy_r,\end{aligned} \tag{15}$$

where $\bar{S}_{x_r y_r}$ is given in Eq. (12).

3.2.2. General case: multiple riders

The previous section focuses on the case with just one rider in the system. In such a case, if the rider is located in the feasible region of a driver, this driver will always agree to match since there are no other potential matches for the driver. However, when the carpool system gets popular and more riders sign up for the system, it is possible that a driver can receive multiple requests that are financially feasible. In this scenario, the probability of the driver's selection of one specific rider is not 100%, which will greatly change the probability of matching for riders and thus the match rate of the system.

Therefore, this section fuses the influence of the driver's selection into formulas of the match rate and system surplus discussed above. When there are multiple riders and multiple drivers in the system, we consider the number of each category to be n_r and n_d, respectively. To maintain simplicity, we assume that the driver has an equal probability of selecting each rider within the feasible region.

Probability of selection

When multiple riders can be matched by the same driver, the probability that the driver selects the specific rider is p_{select}. This denotes the conditional probability of the event H_1*: {the driver selecting this specific rider*}, contingent on the event H_2*: {a specific rider is feasible for a specific driver*}:

$$p_{select} = \frac{P(H_1 \cap H_2)}{P(H_2)} = \frac{\sum_{n_k=1}^{n_r} \frac{1}{n_k} \binom{n_r - 1}{n_k - 1} P^{n_k} (1 - P)^{(n_r - n_k)}}{P}, \tag{16}$$

where P is an abbreviation of the probability of event H_2, calculated with Eq. (13) by assigning $n_d = 1$; n_k is the number of riders who locates in the feasible region of the driver, which could range from 1 to n_r; $P(H_1 \cap H_2)$ is achieved by aggregating

$\frac{1}{n_k}$ weighted by the probability of the occurrence of n_k, which is given by the probability of exactly $(n_k - 1)$ successes in the binomial experiment of $B(n_r - 1, P)$.

Match Rate

The key distinction between the general case and the special case section is the presence of multiple riders, which leads to competition among riders over the same driver. p_{select} is applied to estimate this competition effect and derive the rider's probability of matching and the system's match rate in the general case.

The probability of a rider being matched when there are n_r riders and n_d drivers is expressed as $p_r(n_r, n_d)$, which is the probability of the event *H: {At least 1 driver exists who is in $\Omega_r(X_r, Y_r)$ and agrees to match}*. Let $N_{\Omega,\,yes}$ denote the number of such drivers, then $p_r(n_r, n_d)$ can be expressed as $p(N_{\Omega,\,yes} \geqslant 0)$. Therefore, the expected value of this probability, denoted as $\bar{p}_r(n_r, n_d)$, is expressed as:

$$\begin{aligned}\bar{p}_r(n_r,n_d)=\bar{p}(N_{\Omega,\,yes}\geqslant 0)&=\iint_{A_1} p(X_r=x_r,Y_r=y_r)\,p(N_{\Omega,\,yes}\geqslant 0|X_r=x_r,Y_r=y_r)\,dx_r dy_r\\&=\int_0^{\frac{\sqrt{A}}{2}}\int_0^{\frac{\sqrt{A}}{2}} f_{X_r,Y_r}(x_r,y_r)\left[1-\left(1-\iint_{\Omega_r(x_r,y_r)} f_{X_d,Y_d}(x_d,y_d)dx_d dy_d\, p_{select}\right)^{n_d}\right]dx_r dy_r,\end{aligned} \tag{17}$$

where $p(N_{\Omega,\,yes} \geqslant 0|X_r = x_r, Y_r = y_r)$ is derived with $A_f(x_r, y_r)$ provided in Table 1 and p_{select} provided in Eq. (16).

Consequently, the system's match rate when there are n_r riders with n_d drivers, denoted as $\bar{p}_{sys}(n_r, n_d)$, can be expressed as:

$$\bar{p}_{sys}(n_r,n_d)=\frac{2n_r}{(n_r+n_d)}\,\bar{p}_r(n_r,n_d). \tag{18}$$

SystemSurplus

The derivation of system surplus in the general case share the same logic with the special case but with the incorporation of the probability of selection, p_{select}.

The expected value of system surplus when there are n_r riders and n_d drivers, denoted as $\bar{S}_{sys}(n_r, n_d)$, is expressed in Eq. (19). In this scenario, the total surplus is the multiplication of the number of riders and the weighted sum of $\bar{S}_{x_r y_r}$ across all possible riders' locations.

$$\begin{aligned}\bar{S}_{sys}(n_r,n_d)&=\frac{n_r}{(n_r+n_d)}\iint_{A_1} p(X_r=x_r,Y_r=y_r)\,\bar{S}_{x_r y_r}\,p(N_{\Omega,\,yes}\geqslant 0|X_r=x_r,Y_r=y_r)dx_r dy_r\\&=\frac{n_r}{(1+n_d)}\iint_{A_1} f_{X_r,Y_r}(x_r,y_r)\,\bar{S}_{x_r y_r}\left[1-\left(1-\iint_{\Omega_r(x_r,y_r)} f_{X_d,Y_d}(x_d,y_d)dx_d dy_d\, p_{select}\right)^{n_d}\right]dx_r dy_r.\end{aligned} \tag{19}$$

3.3. Flexible-role carpool system

This section derives measures of performance under the case where travelers do not have pre-assigned roles. In this case, each traveler can be either a driver or rider, depending on if that helps them find a match. This provides more flexibility for the users.

Expanding upon the formula developed in the previous section, a tree model is employed to represent this flexible system. Moreover, to explore opportunities for crafting more efficient and generative models, the tree pruning method is introduced. The structure of this tree is shown in Fig. 3. Nodes are the fundamental units from which trees are constructed. Each node has a unique state vector, denoted as $v(v_1, v_2, v_3)$, which encapsulates the number of agents in the system currently:

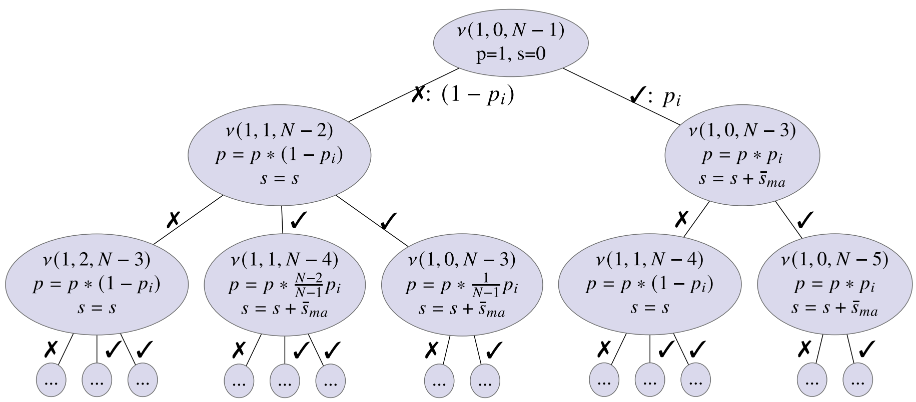

Fig. 3. Tree structure for flexible-role carpool matching system.

- v_1 represents the number of agents in a searching state as riders, and at most 1 agent at a time can be searching for carpool pairs.
- v_2 is the number of agents in the driver-only pool who were unsuccessful in finding matches as riders but are waiting for potential matches as drivers.
- v_3 presents the number of agents in the flexible-role pool, who has not been assigned a role yet and are available for matching with either role.

Let N be the total number of travelers in the system. The state vector at the root node is $v(1, 0, N-1)$, which means from the beginning of the matching process, a traveler is randomly selected to be a rider and searches for a match, regarding the rest $N-1$ flexible agents as drivers. If there is any agent presented in v_2, there will be 3 directed edges emanating from this parent node since the matched driver can originate from both v_3 and v_2; if not, there will be 2 directed edges from it. Then if this searching rider is successfully matched, denoted by the right branches from the parent node, both the rider and the corresponding driver (selected from either v_2 or v_3) are removed from the system; however, if a match is not found, denoted the left branch, the searching rider is placed in the driver-only pool, v_2, to await potential matches, and one agent out of v_3 will be moved to v_1 to search. Repeat this process until the system is empty or there are only drivers left, which implies that at the leaf node, v_1 and v_3 are always 0. For the latter scenarios, all drivers will leave the system by driving alone.

Therefore, the height of this tree equals the number of all agents (N) within the carpool system, representing the length of the path from the root node to the deepest leaf node. The depth of the leaf tree, h_i, varies within $\left[\lfloor \frac{N}{2} \rfloor, N\right]$. The maximum depth of the path is N when no one in the system is matched, and the minimum depth $\lfloor \frac{N}{2} \rfloor$ when the maximum number of travelers is matched.

The likelihood shown along the edge is the conditional probability from its parent node; and p_i is the probability of the i^{th} served agent getting matched with the appearance of n_i drivers, which is the abbreviation of $\bar{p}_r(1, n_i)$. In each node, the probability value, p, denotes the likelihood of this current state (following the path from the root node to this node); s denotes the total surplus out of the whole system at this current state. Both p and s are derived iteratively, and updated at each layer of the tree. $\bar{s}_{ma}$ is the expected surplus that a matched pair can achieve, which is:

$$\bar{s}_{ma} = \iint_{A_1} f_{X_r,Y_r}(x_r, y_r) \iint_{\Omega_r(x_r,y_r)} f_{X_d,Y_d}(x_d, y_d)\, S(x_r, y_r, x_d, y_d)\, dx_d\, dy_d dx_r dy_r. \tag{20}$$

<u>MatchRate</u>

With the information from the leaf nodes of the tree model, the system's match rate with N flexible-role agents in the system could be derived, which is denoted as $\bar{p}_{sys}(N)$. This is calculated by dividing the weighted average number of matched agents (weighted by the probability at the leaf node) by the number of agents in the system:

$$\bar{p}_{sys}(\mathrm{N}) = \frac{1}{N} \overbrace{\sum_{n_m=1}^{\lfloor \frac{N}{2} \rfloor} \sum_{\sum \delta_i = n_m}}^{\Sigma\pi} \left\{ \underset{\sim}{(2n_m)}^{n_{leaf}} \overbrace{\prod_{i=1}^{h_i} \left[\delta_i * \bar{p}_r(1, n_i) + (1-\delta_i) * (1 - \bar{p}_r(1, n_i))\right]}^{p_{leaf}} \right\},$$
$$\delta_i = \begin{cases} 1, & i^{th} \text{ agent matched} \\ 0, & n_i = 0 \text{ or } i^{\text{th}} \text{ agent not matched} \end{cases} \tag{21}$$
$$n_i = \begin{cases} N, & i = 1 \\ min(0, n_{i-1}), & i > 1 \text{ and if } (i-1)^{\text{th}} \text{ agent not matched} \\ min(0, n_{i-1} - 2), & i > 1 \text{ and if} (i-1)^{\text{th}} \text{ agent matched} \end{cases}$$

where $\sum \pi$ controls the sum along all paths by traversing n_m, the number of matched pairs in each path, in the range of $\left[1, \frac{N}{2}\right]$. p_{leaf} denotes the probability at the leaf node of each path, given by the continuous multiplication of the probability besides the edge along this path, with either $\bar{p}_r(1, n_i)$ (matched) or $1 - \bar{p}_r(1, n_i)$ (unmatched). n_{leaf} is the number of matched agents at the leaf node of each path. Other variables are explained as follows:

δ_i: An indicator whether the i^{th} agent gets matched, and $\sum_{i=1}^{h_i} \delta_i = n_m$.

n_i: The number of potential 'drivers' in the system, which is also the summation of v_2 and v_3.

n_m: The number of matched pairs along each path, which can not exceed $\lfloor \frac{N}{2} \rfloor$.

h_i: The depth of each path, varies within $\left[\lfloor \frac{N}{2} \rfloor,\ N\right]$.

$\bar{p}_r(1, n_i)$: The probability of a rider being matched with the appearance of n_i drivers.

<u>SystemSurplus</u>

The expected system surplus for a flexible-role system with N agents can also be derived with the information from the leaf nodes of the tree model, denoted as $\bar{S}_{sys}(N)$. This value is given by dividing the weighted average of the total surplus (weighted by the probability at the leaf node) by the number of agents in the system:

$$\bar{S}_{sys}(N) = \frac{1}{N} \overbrace{\sum_{n_m=1}^{\lfloor \frac{N}{2} \rfloor} \sum_{\sum \delta_i = n_m}}^{\Sigma\pi} \left\{ \overbrace{\prod_{i=1}^{h_i} [\delta_i * \bar{p}_r(1, n_i) + (1 - \delta_i) * (1 - \bar{p}_r(1, n_i))]}^{p_{leaf}} * \overbrace{\left(\sum_{i=1}^{h_i} \delta_i * \bar{s}_{ma} \right)}^{s_{leaf}} \right\}, \quad (22)$$

where s_{leaf} is the total surplus achieved at the leaf node of each path, given by the sum of $\bar{s}_{ma}$, the average surplus of all matched carpool pairs, along the path; $\bar{s}_{ma}$ is calculated with Eq. (20).

Tree Pruning

Generating tree models would require significant computational resources and memory usage, which negates the benefits of a simple analytical model. The increase in the number of agents in the system, N, would lead to an exponential growth in the number of leaf nodes. However, certain leaf nodes may exhibit an extremely low probability of occurrence, making their consideration inefficient given the computational resources required. In light of this, a trade-off might be practical: sacrificing a bit of accuracy by cutting off subtrees for the inclusion of a broader scope of agents in the system, enhancing overall representatives. Consequently, we implement a strategy where if the probability, p, of a specific child node falls below a predetermined threshold, ϵ, the subtree originating from that node is pruned. After the pruning process, the leave nodes are different from the original tree, and the match rate and the system surplus can be calculated with Equation (21) and Equation (22).

4. Numerical validation

The validity of the analytical models is assessed using agent-based simulations. We establish two distinct scenarios, fixed and flexible roles scenarios, each defined by conditions as follows. The parameters utilized in these simulations are detailed comprehensively in Table 2.

(1) For fixed-role scenarios, riders and drivers are generated randomly. A rider is randomly chosen to search for carpool pairs among the available drivers. If multiple feasible drivers are found, one is randomly selected for pairing. Successful matches result in both participants being removed from the system, while unmatched riders exit to drive alone, and unmatched drivers remain for potential future pairings. This process repeats until no drivers or riders are left. The match rate is computed as the ratio of matched travelers to the total number of travelers, and the system surplus is calculated by dividing the total surplus by the number of agents.

(2) For flexible-role scenarios, all travelers are generated at random locations. First, an agent is randomly selected and treated as a rider. A rider searches for a match with other agents in the system, who are seen as drivers by this rider. If there are multiple feasible agents for this searcher, one is randomly selected for matching. If matched, both agents are removed from the system. Unmatched agents stay in the system with a driver-only role, awaiting future potential matches. The process continues until only driver-only agents remain or all possible agents are matched. The remaining agents would drive alone. Match rates and system surplus are calculated similarly to the fixed-role scenario.

4.1. Results of tree model

The validation results for the tree model are depicted in Fig. 4. Arranged from left to right, the three columns display results for the fixed-role scenarios with one rider and 1∼10 drivers, five riders and 1∼10 drivers; and the flexible-role scenario with 1∼10 agents. The horizontal axis represents the simulated results, while the vertical axis shows the analytical results. The top row illustrates the match rate, and the bottom row demonstrates the system surplus. In the plot, various colors indicate the number of drivers (or travelers) in the fixed-role (or flexible-role) scenarios. Each color category includes multiple dots, each signifying a different payment-cost ratio.

Fig. 4 shows that the analytical results match well with the simulated results overall: For the fixed-role general case (example of 5 riders and 1∼10 drivers), on average the absolute difference of match rate observed is 1.4%, and the largest abso-

Table 2
Simulation settings.

Notation	Description	Value
A	Network size, the area of the square region (km^2)	100
l	Half the side length of the region (km)	5
λ	Trip generating rate of region (per unit time & area)	[0.01,0.2]
n_d	Number of drivers in the system	[1,10]
n_r	Number of riders in the system	[1,10]
n_f	Number of flexible-role agents in the system	[1,20]
α	Unit cost for driving alone ($/km)	1
β	Unit payment being carried ($/km)	[0.1,1]
γ	payment-cost ratio, derived by (β/α)	[0.1,1]
Iteration	Number of simulations with different random seeds	50000

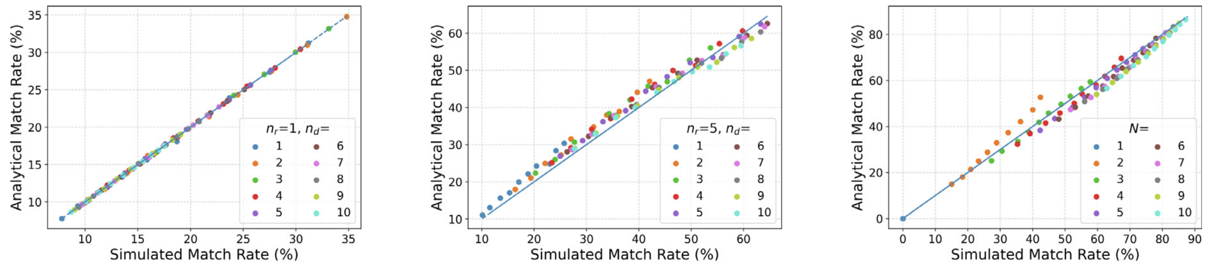

(a) **Match Rate (Fixed-role, $n_r = 1$)** (b) **Match Rate (Fixed-role, $n_r = 5$)** (c) **Match Rate (Flexible-role)**

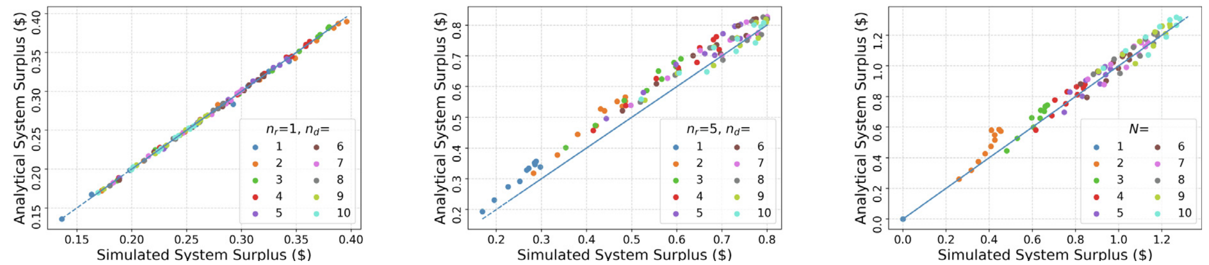

(d) **Surplus (Fixed-role, $n_r = 1$)** (e) **Surplus (Fixed-role, $n_r = 5$)** (f) **Surplus (Flexible-role)**

Fig. 4. Numerical validation for metrics in the Analytical Model.

lute difference is around 5%. The average absolute difference of the system surplus is $ 0.04. The average relative difference observed is 8%, and the largest relative difference observed is 19%. For the flexible-role case (example of 1∼10 agents), on average the absolute difference of match rate observed is 2.6%, and the largest absolute difference observed is 10%, where the analytical model is underestimating the match rate compared with the simulation. The average absolute difference of system surplus observed is $ 0.05, the average relative error observed is 5.5%, and the largest relative error observed is around 24%, which appears when there are only 2 agents.

However, in the fixed-role general scenario, the analytical results slightly overestimate the match rate and surplus. A possible reason is the insufficient consideration of the dependence of matching between riders. Remember we use the feasible region, Ω, to capture the probability of a rider being matched. The 1st rider's not matching with a driver indicates the driver located at the complement of the 1st rider's feasible region, Ω_1'. Conditionally, whether the 2nd rider can be matched with this driver should use the area of $\Omega_1' \cap \Omega_2$, which is a subset of Ω_2. However, in our model, we still use Ω to capture the probability of the consequent rider being matched with this driver regardless of previous information. Therefore, our analytical model overestimates the system performance a bit in this scenario.

Another observation under the flexible-role scenario, from Fig. 4(c), is that when the payment-cost ratio is higher, the model tends to overestimate the match rate a bit. This trend is particularly evident at the tail of the sequence of the orange dots (γ ranges from 0.1 to 1). The underlying cause of this overestimation lies in the expansion of the feasible region as γ increases. A larger γ results in a more extensive overlapping of riders' feasible regions, thereby intensifying their interactions. Similar to the previous observation, the model's limited consideration of the interdependencies in rider matching contributes to this overestimation.

4.2. Results of pruned tree model

In this section, we consider the results of the pruned tree model when the probability threshold, ϵ, is set as 0.0001. The comparative analysis of node counts and performance metrics for both tree models is presented in Table 3. The fourth column of the table quantifies the reduction in node count, expressed as a percentage, indicating the efficiency achieved through pruning. Furthermore, the seventh and last columns detail the accuracy of the pruned model, providing insights into the trade-offs between model simplicity and predictive precision. For example, when there are 20 agents in the system, the pruned tree model reduces around 99.9% of the nodes in the tree model, however, maintains around 94.4% of the accuracy in both the match rate and the system surplus.

Table 3
Original tree and pruned tree comparison.

Agents	Node Count			Match Rate			Suplus		
	Original	Pruned	(%)	Original	Pruned	(%)	Original	Pruned	(%)
2	5	5	100	0.2881	0.2881	100	0.576	0.576	100
4	23	23	100	0.5128	0.5129	100	1.026	1.026	100
6	111	111	100	0.6275	0.6274	100	1.255	1.255	100
8	561	557	99.29	0.6983	0.6982	99.99	1.397	1.396	99.99
10	2925	1935	66.15	0.7466	0.7460	99.92	1.493	1.492	99.92
12	15567	3998	25.68	0.7818	0.7746	99.08	1.564	1.549	99.08
14	84031	5942	7.07	0.8086	0.7929	98.07	1.617	1.586	98.07
16	458305	7596	1.66	0.8296	0.8023	96.70	1.659	1.605	96.70
18	2519285	9073	0.36	0.8466	0.8098	95.66	1.693	1.620	95.66
20	13934183	10328	0.07	0.8606	0.8124	94.40	1.721	1.625	94.40

Nonetheless, a method for selecting certain pivotal probability thresholds, ϵ, remains unexplored. This threshold is connected to the number of agents in the system and plays a significant role in balancing the trade-off between model accuracy and simplicity. The intricacies of determining ϵ are reserved for future investigation. Moving forward, the next section will pivot back to the outcomes and findings from the original analytical model.

5. Results of analytical models

In this section, we examine the impact of various factors on the carpool system's performance under both fixed-role and flexible-role scenarios. Specifically, we focus on understanding how demand, driver-rider ratio, and payment-cost ratio contribute to the overall effectiveness of the system. Additionally, we compare the outcomes between the two distinct scenarios.

5.1. Influence of demand

This section evaluates the system's performance under varying demand conditions under fixed-role system. Fig. 5(a) and Fig. 5(b) illustrate the relationship between the match rate, system surplus, and the number of agents (n_d and n_r, respectively), with the payment-cost ratio fixed at 0.5.

In Fig. 5(a) and Fig. 5(b), the data generally exhibit an unimodal trend. Both the match rate and system surplus escalate as the number of drivers surpasses the number of riders, peaking when the driver count marginally exceeds that of the riders, before commencing a decline. This ascent is attributed to a shortfall in one group (n_r or n_d) relative to the other's demand (n_d or n_r), signaling an imbalance. In contrast, the descent signifies a scenario where supply oversteps demand, leading to oversupply. The dynamics of this rise and fall, governed by the interplay of driver and rider demand, are further expounded in the subsequent section.

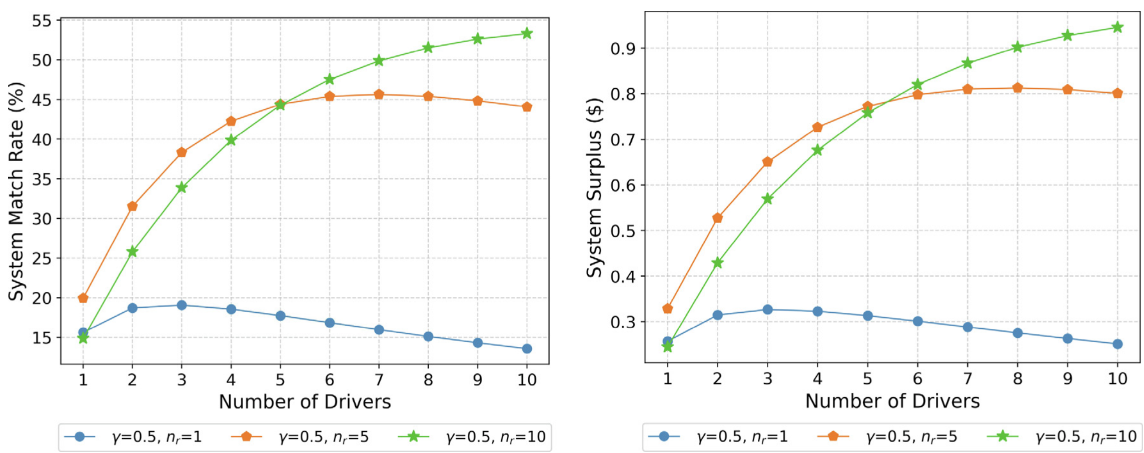

(a) **Match Rate** (b) **System Surplus**

Fig. 5. System performance with the changes in demand.

5.2. Influence of driver-rider ratio

This section examines the impact of the driver-rider ratio on system performance. We consider both fixed-role scenarios with varying driver-rider ratios and a flexible-role scenario with equally numbered drivers and riders. Throughout, the total number of travelers is held constant at 20. Also, different payment-cost ratio sets are provided, as illustrated in Fig. 6(a) and Fig. 6(b).

Fig. 6(a) illustrates the match rate with more riders with fewer drivers, indicating a reduced driver-rider ratio. The figure includes fixed-role scenarios with three payment-cost ratios (γ) and a flexible-role scenario. The highest match rate in fixed-role scenarios is reached when the driver-rider ratio is one-to-one, signifying equilibrium. Additionally, the steeper slope observed at $\gamma = 0.7$ compared to $\gamma = 0.5$ indicates that changes in the driver-rider ratio have a more pronounced impact at higher γ values. This is because a higher γ lessens the payment's restrictiveness in covering driver costs, making equilibrium more sensitive to ratio changes. Notably, the flexible-role system (blue horizontal line) achieves a higher match rate than the fixed-role system at $\gamma = 0.5$ (blue curve), highlighting the benefits of role flexibility, detailed in the final subsection.

Fig. 6(b) demonstrates system surplus variations, the flexible-role system's surplus exceeds that of the fixed-role system, owing to agents' role flexibility. Analysis of fixed-role scenarios indicates that the highest system surplus also occurs at a one-to-one driver-rider ratio under our test scenario, emphasizing the importance of this equilibrium.

5.3. Influence of payment-cost ratio

In this analysis, we compare the impact of the payment-cost ratio (γ) on system performance in fixed-role and flexible-role scenarios, maintaining an equal number of agents in both scenarios. Fig. 7(a) and Fig. 7(b) show the relationship between γ and both the match rate and system surplus, across different payment-cost ratios (γ).

Fig. 7(a) reveals that as γ increases, the match rate also increases, with the flexible-role system surpassing the fixed-role system. Contrarily, Fig. 7(b) indicates that the highest system surplus does not correlate with the highest γ. The surplus initially increases but then starts to decrease beyond a certain γ value. This decline is due to the trade-off between increased match rates and the expected surplus for matched pairs. Higher γ values expand the feasible region, raising match probabilities; but also mean greater average distances between the rider and feasible drivers, resulting in longer detours and lower expected surplus for matched pairs. Hence, it explains the initial rise and subsequent fall of system surplus as γ increases.

5.4. Evaluating performance: fixed-role vs. flexible-role systems

The preceding results indicate that a driver-rider ratio of one yields the optimal performance in the fixed-role system. Consequently, we employ this ratio setting to assess and compare the performance between the fixed-role and flexible-role systems.

In Fig. 8(a) and Fig. 8(b), both systems employ a one-to-one driver-rider ratio and a payment-cost ratio of 0.5, with the total agent count ranging from 2 to 20. In both figures, the flexible-role system consistently outperforms the fixed-role system, additionally, the initial slope of the flexible-role system is marginally steeper compared to the fixed-role system. These advantages are attributed to the agents' flexibility in role assumption. For instance, agents located far from their destination might seldom be chosen as riders but could effectively serve as drivers, picking up riders en route. Flexible-role selection enables such agents to participate more actively, thereby boosting the system's overall efficiency.

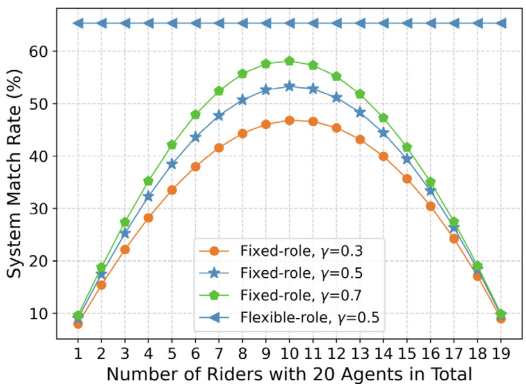

(a) **Match Rate**

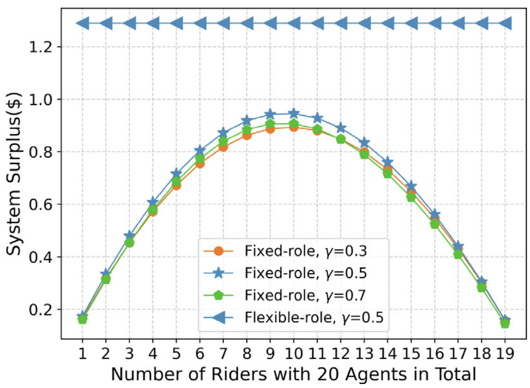

(b) **Surplus**

Fig. 6. System performance with the changes in driver-rider ratio.

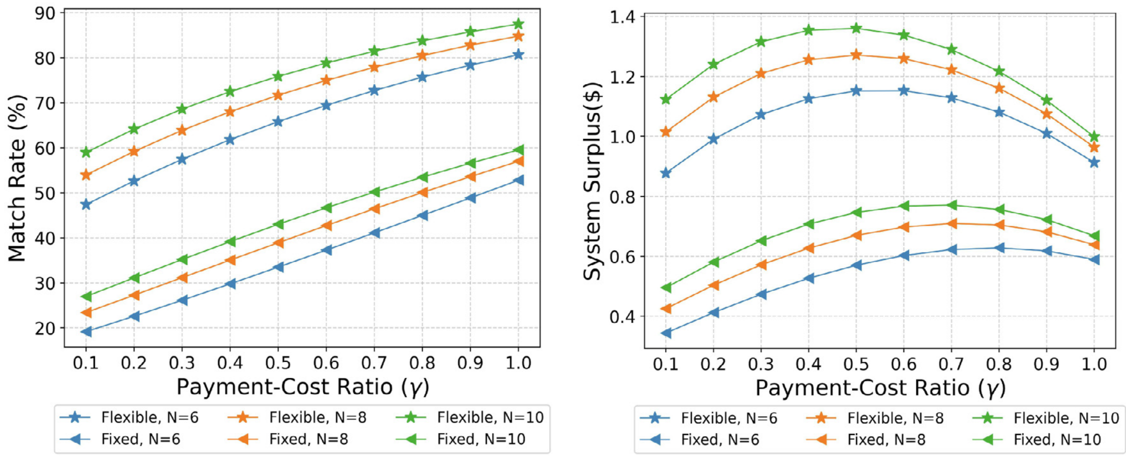

(a) **Match Rate** (b) **System Surplus**

Fig. 7. System performance with the changes in payment-cost ratio.

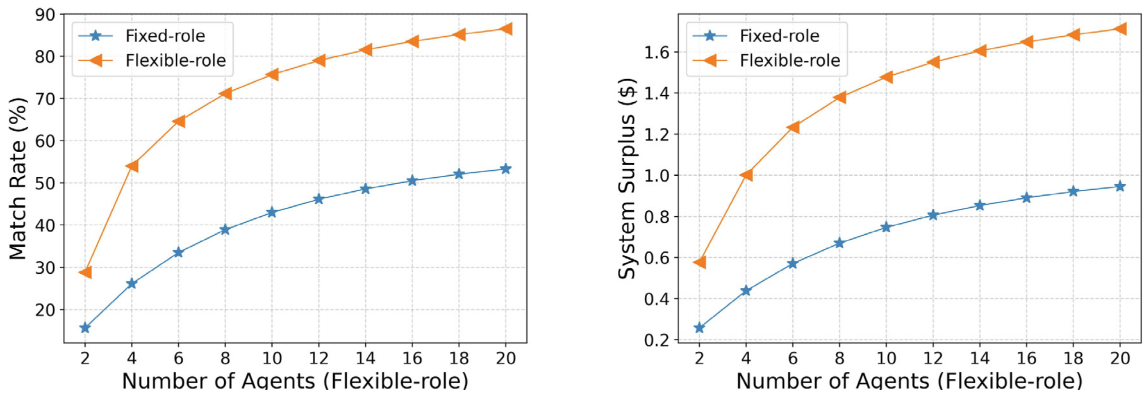

(a) **Match Rate** (b) **System Surplus**

Fig. 8. System performance of fixed-role and flexible-role system.

6. Concluding remarks

This paper presents an innovative analytical model designed for predicting the performance of carpool systems in a grid-structured, square city characterized by a homogeneous, many-to-one demand pattern. The proposed model underscores the cost-based detour limit, which not only ensures individual rationality and system sustainability but also provides critical insights under more realistic carpooling behavior. These insights are instrumental for stakeholders in evaluating the potential return on investment in a carpool system. Numerical experiments are conducted and validate the results from the analytical model under both fixed-role and flexible-role scenarios.

Overall, the findings from the proposed models show a strong correlation with the validating experiment results. Consistent with the concept of the economies of scale, an increase in participant numbers typically elevates the average system surplus; and boosts the likelihood of successful matches, also evidenced by Lehe et al. (2021) and Liu et al. (2023). In scenarios with a specific total number of fixed-role agents, optimal match rates and surpluses are typically achieved when riders and drivers are equally represented under our test settings. The results emphasize the significant benefits of flexible roles in increasing the likelihood of matching and system surplus compared with the fixed role scenarios. This highlights the importance of motivating travelers to opt for flexible roles, thereby balancing demand and supply effectively.

Several limitations and future research directions should be mentioned: First, this study emphasizes the financially feasible rule considering the cost-based detour limits, ignoring the maximum waiting time constraints. This approach, however, becomes less practical in a larger region where agents are more sparsely distributed. The inclusion of a maximum wait time constraint could be incorporated via an additional boundary condition to the feasible region. For example, the feasible region described in Equation11 could be extended to $\Omega T_r(X_r, Y_r) = \Omega_r(X_r, Y_r) \cap \{(X_d, Y_d)|(|X_r - X_d| + |Y_r - Y_d|) \leqslant \Delta\}$, where the second set is the additional boundary introduced by the wait time constraint Δ. This results in more complex discussions regarding the relative relationship among variables. Future studies could consider this extension based on the model in this paper. Second, generating tree models under the flexible-role scenario would require significant computational resources and memory usage, which negates the benefits of a simple analytical model. Tree-pruning method for the inclusion of a broader scope of agents in the system based on a probability threshold is introduced to reduce the complexity with a compromise on accuracy. However, the selection of the threshold remains unexplored in this paper. Additionally, there is scope to investigate a dynamic threshold that adjusts according to different conditions or parameters, potentially optimizing the model's performance and adaptability. Other future enhancements to the model may also include batch assignments at each level of the tree to streamline the process instead of assigning agents one after another. Third, the model assumes a square city layout with homogeneous demand, which may not accurately reflect the complexities of real-world transportation networks and diverse demand patterns. Exploring the model with heterogeneous demand distribution is indeed a potential extension of this work. Expanding the model from a many-to-one to a many-to-many system, encompassing multiple origins and destinations, is another crucial area for exploration. Fourthly, the development of closed-form formulas for system performance considering system optimal matching of riders to drivers is an opportunity for further investigation. Lastly, this paper does not consider individual preference, in either the process of a driver selecting a rider, or a rider selecting a driver. However, our result provides a lower bound for the maximum match rate and surplus the system can achieve. The potential impact of this greedy selection of travelers warrants further investigation in future research. These improvements would provide planners and stakeholders with a more comprehensive analytical model with versatility and applicability.

Author contributions

The authors confirm contribution to the paper as follows: study conception and design: X. Dong, H. Liu, V. Gayah; simulation: X. Dong; analysis and interpretation of results: X. Dong, H. Liu, V. Gayah; draft manuscript preparation: X. Dong, H. Liu, V. Gayah; All authors reviewed the results and approved the final version of the manuscript.

Declaration of Competing Interest

The authors declare that they have no known competing financial interests or personal relationships that could have appeared to influence the work reported in this paper.

Acknowledgements

This research was supported by NSF Grants CMMI-2052337.

References

Cervero, R., 2003. Road expansion, urban growth, and induced travel: a path analysis. J. Am. Plan. Assoc. 69 (2), 145–163.
Daganzo, C.F., Ouyang, Y., 2019. A general model of demand-responsive transportation services: from taxi to ridesharing to dial-a-ride. Transport. Res. Part B: Methodol. 126, 213–224.
Daganzo, C.F., Ouyang, Y., Yang, H., 2020. Analysis of ride-sharing with service time and detour guarantees. Transport. Res. Part B: Methodol. 140, 130–150.
Furuhata, M., Dessouky, M., Ordóñez, F., Brunet, M.-E., Wang, X., Koenig, S., 2013. Ridesharing: the state-of-the-art and future directions. Transport. Res. Part B: Methodol. 57, 28–46.
Handke, V., Jonuschat, H., 2012. Flexible ridesharing: new opportunities and service concepts for sustainable mobility. Springer Science & Business Media.
Huang, S.-C., Jiau, M.-K., Lin, C.-H., 2014. A genetic-algorithm-based approach to solve carpool service problems in cloud computing. IEEE Trans. Intell. Transport. Syst. 16 (1), 352–364.
Lam, W.H., Huang, H.-J., 1995. Dynamic user optimal traffic assignment model for many to one travel demand. Transport. Res. Part B: Methodol. 29 (4), 243–259.
Lehe, L., Gayah, V.V., Pandey, A., 2021. Increasing returns to scale in carpool matching: evidence from scoop. Transp. Find.
Lin, Y., Li, W., Qiu, F., Xu, H., 2012. Research on optimization of vehicle routing problem for ride-sharing taxi. Proc.-Soc. Behav. Sci. 43, 494–502.
Liu, H., Devunuri, S., Lehe, L., Gayah, V.V., 2023. Scale effects in ridesplitting: a case study of the city of chicago. Transport. Res. Part A: Policy Pract. 173, 103690.
Masoud, N., Jayakrishnan, R., 2017a. A decomposition algorithm to solve the multi-hop peer-to-peer ride-matching problem. Transport. Res. Part B: Methodol. 99, 1–29.
Masoud, N., Jayakrishnan, R., 2017b. A real-time algorithm to solve the peer-to-peer ride-matching problem in a flexible ridesharing system. Transport. Res. Part B: Methodol. 106, 218–236.
Mortazavi, A., Ghasri, M., Ray, T., 2024. Integrated demand responsive transport in low-demand areas: a case study of Canberra, Australia. Transport. Res. Part D: Transp. Environ. 127, 104036.
Olsson, L.E., Maier, R., Friman, M., 2019. Why do they ride with others? meta-analysis of factors influencing travelers to carpool. Sustainability 11 (8), 2414.
OpenDataDC, 2023, 'Single member district in d.c.', https://opendata.dc.gov/datasets/single-member-district-from-2023.
Ouyang, Y., Yang, H., Daganzo, C.F., 2021. Performance of reservation-based carpooling services under detour and waiting time restrictions. Transport. Res. Part B: Methodol. 150, 370–385.
Regue, R., Masoud, N., Recker, W., 2016. Car2work: Shared mobility concept to connect commuters with workplaces. Transp. Res. Rec. 2542 (1), 102–110.
Su, Q., Wang, D.Z., 2020. On the morning commute problem with distant parking options in the era of autonomous vehicles. Transport. Res. Part C: Emerg. Technol. 120, 102799.

Tafreshian, A., Masoud, N., 2020. Trip-based graph partitioning in dynamic ridesharing. Transport. Res. Part C: Emerg. Technol. 114, 532–553.
Tian, Q., Liu, P., Ong, G.P., Huang, H.-J., 2021. Morning commuting pattern and crowding pricing in a many-to-one public transit system with heterogeneous users. Transport. Res. Part E: Logist. Transport. Rev. 145, 102182.
U.S. Census Bureau, 2022. 'American community survey (acs)', https://www.census.gov/programs-surveys/acs.
Wang, H., Meng, Q., Zhang, X.-N., 2015. Optimal parking pricing in many-to-one park-and-ride network with parking space constraints. Transp. Res. Rec. 2498 (1), 99–108.
Wang, J., Wang, X., Yang, S., Yang, H., Zhang, X., Gao, Z., 2021. Predicting the matching probability and the expected ride/shared distance for each dynamic ridepooling order: A mathematical modeling approach. Transport. Res. Part B: Methodol. 154, 125–146.
Xia, J., Curtin, K.M., Li, W., Zhao, Y., 2015. A new model for a carpool matching service. PloS one 10 (6).
Zhang, D., He, T., Liu, Y., Lin, S., Stankovic, J.A., 2014. A carpooling recommendation system for taxicab services. IEEE Trans. Emerg. Top. Comput. 2 (3), 254–266.
Zhang, D., Li, Y., Zhang, F., Lu, M., Liu, Y., He, T., 2013. coride: Carpool service with a win-win fare model for large-scale taxicab networks. In: Proceedings of the 11th ACM conference on embedded networked sensor systems, pp. 1–14.
Zhang, W., He, R., Chen, Y., Gao, M., Ma, C., 2019. Research on taxi pricing model and optimization for carpooling detour problem. J. Adv. Transport.